Polymer 51 (2010) 5997–6004

Contents lists available at ScienceDirect

Polymer

journal homepage: www.elsevier.com/locate/polymer

Novel water and oil repellent POSS-based organic/inorganic nanomaterial: Preparation, characterization and application to cotton fabrics

Yu Gao [a], Chuanglong He [a], Yangen Huang [a], Feng-Ling Qing [a,b,*]

[a] College of Chemistry, Chemical Engineering and Biotechnology, Donghua University, 2999 North Renmin Road, 201620 Shanghai, China
[b] Key Laboratory of Organofluorine Chemistry, Shanghai Institute of Organic Chemistry, Chinese Academy of Sciences, 345 Lingling Road, 200032 Shanghai, China

ARTICLE INFO

Article history:
Received 3 July 2010
Received in revised form
1 September 2010
Accepted 12 October 2010
Available online 20 October 2010

Keywords:
Superhydrophobic
Oil repellent
Nanomaterial

ABSTRACT

A series of polyhedral oligomeric silsesquioxane (POSS) based hybrid terpolymers P(POSS-MMA-$(HFPO)_3$MA) were synthesized and characterized by NMR, FT-IR, GPC, DSC and TG. The thermal properties of these terpolymers were improved by the introduction of POSS cage. The cotton fabrics coated with these terpolymers possessed excellent water and oil repellency. The water and salad oil contact angle could be achieved from ~140° to 152° and from ~127° to 144° respectively as the content of POSS in the terpolymer increased from 6.4 wt% to 13.4 wt%. Compared with P(MMA-$(HFPO)_3$MA) copolymer-coated cotton fabrics, POSS-based terpolymer coated cotton fabrics showed better oil repellency with a tendency of first increasing and then decreasing with an increase of the POSS content. The *n*-hexadecane (surface tension: 27.4 mN/m, 20 °C) contact angle reached ~117° for coated cotton fabrics with terpolymer containing 9.5 wt% of POSS.

1. Introduction

Surfaces with water and oil repellency have attracted increasing interest for their applications in diverse fields such as self-cleaning paint, sports and outdoor clothing, biomedical layers, integrated sensors, microfluidic channels [1–4]. Such surfaces are usually achieved by the combination of surface geometrical structure and low surface energy chemical compositions [5]. It is not difficult to realize water repellency because of the high surface tension of water (~72 mN/m). Hydrophobic or even superhydrophobic surfaces achieved by the combination of surface roughening and lowering the surface free energy have been widely reported in recent years [6–10].

In order to achieve oil repellency, the surface free energy of a substrate lower than 20 mN/m is necessary because typical surface tensions of oils are 20–30 mN/m. Several classes of coating materials were developed to meet the requirement of oil repellency, such as fluorinated acrylic polymers, fluorosilicone polymers, fluorinated polyurethane and so on [11–14]. Among them, long-chain perfluoroalkane are widely used to prepare low surface free energy polymers to realize both water repellency and oil repellency [10,15–17].

Recently, some polyhedral oligomeric silsesquioxane (POSS)-incorporated polymer materials have been reported which exhibited higher use temperature, improved mechanical property and enhanced fire retardation than their pristine counterpart [18–20]. A variety of POSS-containing polymers including epoxy [21], polyurethane [22], poly(methyl methacrylate) [23,24], polysiloxane [25], polyethylene/polyethylene oxide [26,27], polypropylene/polypropylene oxide [28,29], polystyrene [30,31], poly norbornene [32] and perfluorocyclobutyl aryl ether copolymers [33], have been prepared via blending or polymerization.

Fluorinated POSS-containing long-chain fluoroalkyl groups blended with polymethyl methacrylate (PMMA) or polyethyl methacrylate (PEMA) have been applied to form water and oil repellent surface [10,34]. The hydrophobicity of epoxy resin containing hepta (3,3,3-trifluoropropyl) POSS-capped poly(3-caprolactone) was also significantly enhanced by the addition of the fluorinated POSS [35]. It is demonstrated that the POSS-containing long-chain fluoroalkyl groups significantly increased water and oil repellency of those materials.

The long-chain fluoroalkyl composites nevertheless are suspected to contain or degrade into fluorinated telomer alcohols and subsequently transform into perfluorocarboxylates including perfluorooctanoate (PFOA), which has been globally detected in wildlife, humans and the environment. Studies suggest that PFOAs, perfluorooctyl sulfonate (PFOS) and other molecules containing perfluoroalkyl chain (C_nF_{2n+1}, $n \geq 8$) could accumulate in wildlife

* Corresponding author. College of Chemistry, Chemical Engineering and Biotechnology, Donghua University, 2999 North Renmin Road, Shanghai 201620, China. Tel.: +86 21 54925187; fax: +86 21 64166128.
E-mail address: flq@mail.sioc.ac.cn (F.-L. Qing).

0032-3861/$ – see front matter © 2010 Elsevier Ltd. All rights reserved.
doi:10.1016/j.polymer.2010.10.020

and human body, which result in a potential risk for human health and environmental concerns [36,37]. Since 2000, the USA Environmental Protection Agency (EPA) has taken various actions to help minimize the potential impact of long-chain perfluorinated chemicals (PFCs) on human health and the environment. Therefore, European Union has restricted the use of PFOS and is evaluating the risks of PFOA exposure.

Fortunately, hydrofluoropolyether has been proved no potential for irritation or skin sensitization, no detectable genotoxic activity *in vitro* or *in vivo*, and no cardiac sensitization potential [38]. Fluoropolyether seem to be the promising substitute for long-chain perfluoroalkane due to their outstanding physical and chemical properties such as high chemical resistance, high lubricating ability, low surface energy and low toxicity [38,39]. Polymer blends, fluorinated hybrids or copolymers based on the presence of fluoropolyether chains are being applied as water and oil repellent [1,14,40–43]. Series copolymers consisting of fluoropolyether and methyl methacrylate (MMA) segment were prepared and shown to give low energy surfaces. The water (surface tension: 72.8 mN/m, 20 °C) and n-hexadecane (surface tension: 27.4 mN/m, 20 °C) contact angle of 112° and 72° was observed respectively on the surface coated with the copolymer containing 50% (mol) fluoropolyether [39]. However, little work has been done on synthesis of fluoropolyether modified POSS or applications of copolymers consisting of fluoropolyether and POSS to construct hydrophobic and oleophobic surface.

In this paper, a new class of environmental friendly fluorinated polymers containing fluoropolyether and POSS groups was prepared via the conventional radical addition polymerization. The composition, thermal properties of the polymers and morphology, wettability of the polymer-coated cotton fabrics were characterized. The possible mechanism and content effect of POSS on water and oil repellency of the coated cotton fabrics were also discussed.

2. Experimental

2.1. Materials

Methyl methacrylate (98%) was purchased from Sinopharm Chemical Reagent Co. Ltd. (Shanghai, China) and distilled from calcium hydride under vacuum before use. 2,2′-azobisisobutyronitrile (AIBN), was also purchased from Sinopharm Chemical Reagent Co. Ltd. and was recrystallized from methanol. Octavinyl polyhedral oligomeric silsesquioxane (Ov-POSS) (99%) was purchased from Shenyang Meixi Fine Chemicals Co. Ltd. (Shenyang, China). The perfluoropolyether, 2,3,3,3-tetrafluoro-2-(1,1,2,3,3,3-hexafluoro-2-(perfluoropropoxy)propoxy) propanoyl fluoride (THPF), was obtained from Shanghai Institute of Organic Chemistry, Chinese Academy of Sciences. The molecular structure of THPF can be represented by the following formula: $CF_3CF_2CF_2OCF(CF_3)CF_2OCF(CF_3)COF$. Lithium aluminium hydride was purchased from Sigma–Aldrich Shanghai Trading Co Ltd. (Shanghai, China). Tetrahydrofuran (THF) was distilled from sodium/benzophenone immediately prior to use. Lithium aluminium hydride, Ov-POSS and other chemicals were used as received without further purification.

2.2. Characterization and measurements

NMR spectra were recorded at ambient temperature on Bruker AV400 operating at 400.1, 376.5 and 79.5 MHz for corresponding ^1H, ^{19}F and ^{29}Si nuclei, respectively. Tetramethylsilane (TMS) was applied as the internal chemical shift reference for ^1H NMR, Downfield shifts are designated as positive. FT-IR spectra were recorded on an FT-IR spectrometer (Avatar 380) using KBr crystal in the infrared region 4000–400 cm^{-1}.

Molecular weight and distribution were determined by gel permeation chromatography (GPC) using a series of three linear Styragel columns. Waters 1515 pump and Waters 2414 differential refractive index (RI) detector (set at 35 °C) were used. The eluent was THF at a flow rate of 1.0 mL/min. A commercial calibration kit of polystyrene standards was utilized to calibrate the GPC elution traces. As a result, the molecular weights (M_w, M_n) and their distributions were thus evaluated.

The sessile drop method was used for static contact angle measurements at ambient temperature with an automatic video contact angle testing apparatus (DataPhysics OCA 40, DataPhysics Instruments GmbH; Germany). The probe liquids were deionized water, n-hexadecane, and n-dodecane. The average CA value was determined by measuring three to five different positions of the same sample with 5 μL each time. The water contact angle (WCA) hysteresis was calculated by $\theta_A - \theta_R$, where θ_A is the advancing contact angle and θ_R is the receding contact angle. The advancing and receding angle were measured by the same instrument at ambient conditions.

The structural and surface morphology of the polymers on cotton fabrics was characterized by field emission scanning electron microscopy (FE-SEM) (S-4800 FE-SEM, Hitachi, Japan).

X-ray photoelectron spectroscopy (XPS) analysis was carried out by using XPS spectroscopy (XPS, XSAM800, Kratos, UK) with a monochromatic AlKα X-ray source (1486.6 eV photons), operated at 180 W (12 kV and 15 mA) and a pressure of 2×10^{-7} Pa. The survey spectra and the detailed C1s spectra were obtained at a photoelectron take-off angle (α, with respect to the sample surface) of 20°.

Differential scanning calorimetry (DSC) was performed under a nitrogen atmosphere on a Netzsch DSC 204 F1 Phoenix. Samples were cooled to −110 °C and heated at a rate of 10 °C/min. Thermogravimetric analyses (TGA) were carried out under N_2 atmosphere with a heating rate of 10 °C/min up to 800 °C by using a Netzsch TG 209 F1 instruments.

2.3. Synthesis of the monomer

2,3,3,3-tetrafluoro-2-(1,1,2,3,3,3-hexafluoro-2-(perfluoropropoxy)propoxy) propyl methacrylate [$(HFPO)_3MA$] was synthesized according to the literature [44] as shown in Scheme 1.

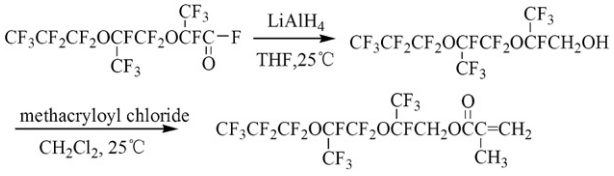

Scheme 1. Synthesis of $(HFPO)_3MA$.

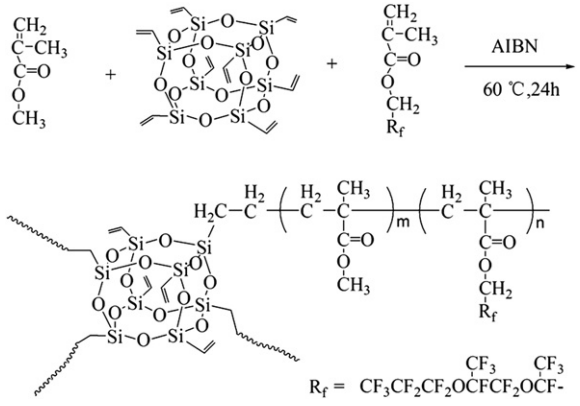

Scheme 2. Preparation of P(POSS-MMA-$(HFPO)_3MA$).

^{1}H NMR (400.13 MHz, $CDCl_3$) δ: 1.96 ppm (s, 3H, $-CH_3$), 4.68 ppm (d, 1H, $-CH_2-$, $^3J_{HF} = 8.0$ Hz), 4.74 ppm (d, 1H, $-CH_2-$, $^3J_{HF} = 7.2$ Hz.), 5.70 ppm (s, 1H, $-CH_2{=}C$), 6.19 ppm (s, 1H, $-CH_2{=}C$).

^{19}F NMR (376.50 MHz, $CDCl_3$) δ: −80.03 to −83.17 (m, 13F, all $-CF_2-O-$ and $-CF_3$ signals), −129.75 (s, 2F, $CF_3-\mathbf{CF}_2-CF_2-$), −133.75 (m, 1F, $-C(CF_3)\mathbf{F}-CH_2-$), −145.17 (m, 1F, $-C(CF_3)\mathbf{F}-CF_2-$). GC/MS (CI, CH_4): $m/z = 551([M + H]^+)$.

2.4. Polymerization of P(POSS-MMA-(HFPO)$_3$MA) polymers

In a typical polymerization procedure, to a three-necked flask fitted with condenser and N_2 inlet, THF (5 mL), MMA (0.3 g, 3 mmol), and Ov-POSS at desired amount were added, followed by 1 wt% AIBN relative to monomers. The solution was stirred and degassed with N_2 for 30 min, and then maintained at 60 °C for 4 h. Subsequently, $(HFPO)_3MA$ (0.8 g, 1.5 mmol) and 1 wt% AIBN were added. The solution was allowed to stir for 20 h at 60 °C followed by dropwise addition into a 10-fold excess of chloroform/methanol ($v/v = 1/30$) under vigorously agitation. The precipitate was then filtered and redissolved in chloroform and reprecipitated in chloroform/methanol ($v/v = 1/30$). This purification procedure was repeated three times. The polymers were finally dried under vacuum at 60 °C to a white powder of constant weight. The polymers with different POSS feed amount of 0, 0.1, 0.15, 0.20 g were labeled by **P1**, **P2**, **P3**, **P4**, respectively. Meanwhile, **PMMA** and **P (MMA-POSS)** (POSS feed ratio: 12.0%) are also prepared for comparison.

2.5. Treatment of the cotton fabrics with the polymers

The desized, bleached and cleaned cotton fabrics (3 cm × 10 cm, about 0.3 g) were soaked in the 0.01 g/mL polymers solution (THF as solvent) for 2 h. The cotton fabrics were dried at 80 °C for 30 min and then cured at 160 °C for 3 min.

3. Results and discussion

3.1. Purification and characterization of terpolymers

The P(POSS-MMA-(HFPO)$_3$MA) terpolymers with different POSS contents were polymerized radically (Scheme 2).

In ^{29}Si NMR spectrum of P(POSS-MMA-(HFPO)$_3$MA) (**P4**) (Fig. 1), the peaks at −79.3 and −65.7 ppm are respectively assigned to the silicon atoms connected to the unreacted and the reacted vinyl groups. The presence of signal at −65.7 ppm confirms that Ov-POSS participated in the polymerization. The number of reacted vinyl groups of all the terpolymers ranged from 3.3 to 3.5 calculated according to the data of elemental analyses of Si and ^{1}H NMR. The residue vinyl groups provide an opportunity for introducing other functional groups into the terpolymers in further applications.

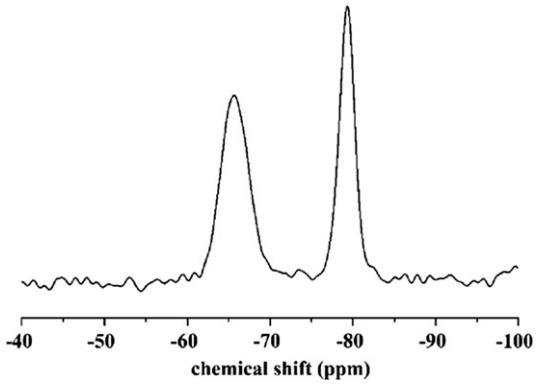

Fig. 1. ^{29}Si NMR spectrum of **P4**.

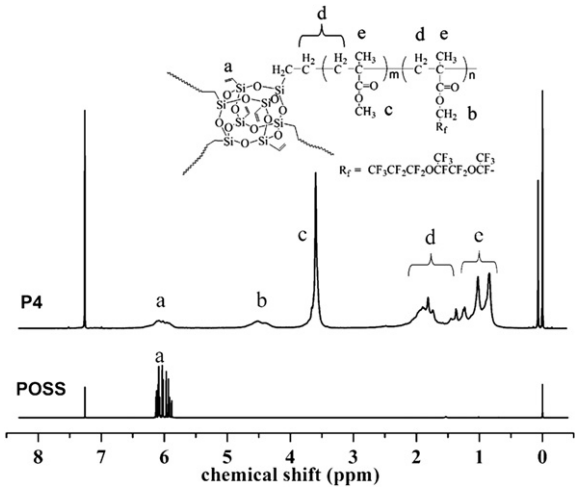

Fig. 2. ^{1}H NMR spectra of pure Ov-POSS and **P4**.

^{1}H NMR spectra of Ov-POSS, P(POSS-MMA-(HFPO)$_3$MA) (**P4**) in chloroform-d were shown in Fig. 2. The resonance band of vinyl protons in pure Ov-POSS is observed at ~6.0 ppm as multiple peaks. For P(POSS-MMA-(HFPO)$_3$MA) (**P4**), the signals at 4.2–4.7 ppm and 3.6 ppm are attributed to methylene and methyl proton connected to ester group in $(HFPO)_3MA$ and MMA, respectively. The proton signals of methylene groups in the polymer backbone are at 1.3–2.2 ppm, while the side methyl groups at 0.7–1.3 ppm, as shown in Fig. 2. The weak peak at ~6.0 ppm indicates the existence of unreacted vinyl group in Ov-POSS segment, which is consistent with the result from ^{29}Si NMR.

A chloroform/methanol ($v/v = 1/30$) solution was applied for removing of unreacted Ov-POSS from the product, because the polymers precipitated in it while Ov-POSS dissolved. The dissolution and precipitation procedure was repeated at least three times. FT-IR spectra of P(POSS-MMA-(HFPO)$_3$MA) (**P2**, **P3**, **P4**) as well as the pure Ov-POSS and P(MMA-(HFPO)$_3$MA) (**P1**) for comparison were presented in Fig. 3. For neat Ov-POSS, the bands around 3100–2900 cm^{-1}, ~1410 cm^{-1} and ~1109 cm^{-1} are assigned to the =C–H, C=C stretching and Si–O–Si stretching, respectively. For all

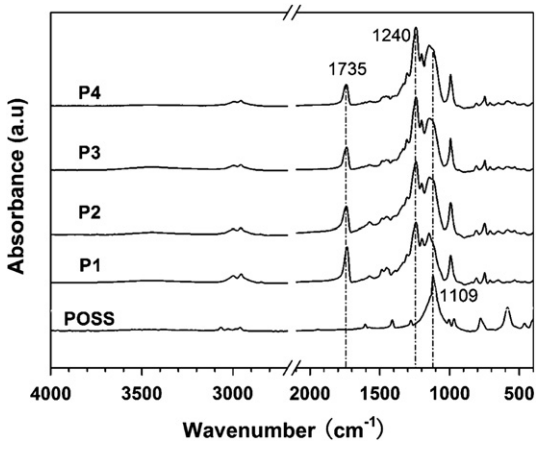

Fig. 3. FT-IR spectra of pure Ov-POSS and P(POSS-MMA-(HFPO)$_3$MA) with different Ov-POSS wt% ratio (**P1**: 0, **P2**: 6.4, **P3**: 9.5, **P4**:13.4).

Table 1
Effect of Ov-POSS Feed Ratio on the results of P(POSS-MMA-$(HFPO)_3$MA).

Sample	POSS (wt%)		Yield (wt%)	M_w ($\times10^3$ g/mol)	M_n ($\times10^3$ g/mol)	PDI (M_w/M_n)	T_g (°C)	T_d[b] (°C)	T_5[c] (°C)	Residue Char[d] (wt%)
	Feed ratio	Product ratio[a]								
P1	0	0	45.5	41.48	39.20	1.06	33.1	154.9	174.0	0.00
P2	8.3	6.4	37.5	17.85	13.46	1.33	44.0	160.1	202.3	5.92
P3	12.0	9.5	30.4	14.05	11.28	1.28	54.6	162.0	219.6	8.41
P4	15.3	13.4	29.2	11.04	9.05	1.22	78.4	231.6	233.6	12.7

[a] Obtained from the elemental analyses of Si.
[b] Onset temperature.
[c] Temperature at weight loss of 5%.
[d] Obtained from TGA.

the polymers, the spectra displayed three major characteristic bands around ~1735 cm^{-1}, ~1240 cm^{-1} and ~1145 cm^{-1} due to C═O, C–F, and C–O–C groups. The stretching absorption bands of $-CH_2$ and $-CH_3$ groups in the polymers are located at 3000–2900 cm^{-1}. The spectra of **P2**, **P3** and **P4** are similar to that of **P1** except that a "double-peak broadened" [45] band from 1150 to 1100 cm^{-1} in all the spectra of P(POSS-MMA-$(HFPO)_3$MA), which may be from the overlap between the characteristic Si–O–Si stretching band of POSS cage and the C–O–C stretching band of P(POSS-MMA-$(HFPO)_3$MA) [45].

The FT-IR features of the mixture of pure Ov-POSS and P(MMA-$(HFPO)_3$MA) (**P1**) are the same as P(POSS-MMA-$(HFPO)_3$MA). The characteristic absorption at 3000–2900 cm^{-1} for $-CH_2$ and $-CH_3$ groups, ~1735 cm^{-1} for C═O, ~1240 cm^{-1} for C–F and the "double-peak broadened" at 1150–1100 cm^{-1} for the overlap of Si–O–Si and the C–O–C stretching band are observed. In order to demonstrate the products are terpolymers in stead of the physical mixtures, the similar dissolution and precipitation procedure was also utilized to the simple physical mixture of pure Ov-POSS and **P1**. The resultant "mixture" was dried in vacuum the same way as for the P(POSS-MMA-$(HFPO)_3$MA) terpolymers and then characterized by FT-IR. As expected, the FT-IR spectrum of the final dried "mixture" is exactly the same as that of pure **P1**, in which the broadened double-peak absorption band from 1150 cm^{-1} to 1100 cm^{-1} didn't appeared. This result demonstrated that the dissolution and precipitation procedure was an effective method to remove the unreacted Ov-POSS [45] and implied that the Ov-POSS was indeed a polymer segment in the polymerization product.

The polymer of P($(HFPO)_3$MA) is insoluble in common organic solvents [39], while the terpolymers of P(POSS-MMA-$(HFPO)_3$MA) show good solubility in THF, chloroform, dichloromethane, toluene and hot acetone. The molecular weights (M_w and M_n) of the terpolymers were measured by GPC and summarized in Table 1. The yield and M_w of the polymer without Ov-POSS (**P1**) is 45.5% and 41480 g/mol, respectively, while for the terpolymer containing 13.4 wt% POSS segments (**P4**), the yield and M_w decreased to 29.2% and 11,040 g/mol. The decrease of yields and molecular weights of products with the increase of POSS contents could be explained by the steric hindrance effect from the bulky POSS group [45].

3.2. Thermal analysis

Thermal properties of the synthesized polymers were studied by thermogravimetric analysis (TGA) and differential scanning calorimetry (DSC). Characterization of the polymers regarding thermal properties is also displayed in Table 1. The glass transition temperature (T_g) increases linearly with increasing POSS content. The T_g is 33.1 °C for P(MMA-$(HFPO)_3$MA) (**P1**) and increases to 78.4 °C after incorporation of 13.4 wt% POSS for P(POSS-MMA-$(HFPO)_3$MA) (**P4**). The reason for the great T_g improvement is probably that the POSS segments dispersed in the terpolymer hindering the motion of P(MMA-$(HFPO)_3$MA) chains in the terpolymer matrix [45]. In a comparison of the thermal stabilities, onset temperature (T_d) and 5 wt% weight loss temperature (T_5) are obtained from TGA. Both T_d and T_5 rise with the increase of POSS content, as seen in Table 2. Moreover, the residue char weight increased with the POSS content also.

Fig. 4(A) shows the weight loss of polymers when heated from ambient (~25 °C) to 800 °C under a nitrogen flow at a heating rate of 10 °C/min. **P1** and **P2** show a three-stage decomposition process, **P3** and **P4** shows a two-stage decomposition process. The initial decomposition of **P1** and **P2** could have been due to the decomposition of PMMA at the head-to-head linkages (the least stable linkages). The second stage of decomposition of **P1** and **P2** was due to the unsaturated chain ends, and the third stage was due to the random scissions along the polymer backbone (the most stable linkages) [46]. As seen from Fig. 4(A) of **P1** to **P4**, with the increase of POSS content, the weight loss attribute to scissions at the head-to-head linkages and the unsaturated chain ends are smaller and smaller and even disappear, the residue char weight increased from 0 to 12.7%. The peak temperatures at which velocity of weight loss reaches maximum (T_m) are displayed in DTG curves (Fig. 4(B)) which have three peak areas. For the first peak area (<250 °C), the peaks weakened with the addition of POSS, and even disappeared when POSS content higher than 13 wt% (seen from **P4**). It means enough POSS can restrain the polymer head-to-head linkages from broking when temperature is lower than 250 °C. For the second (250°–320 °C) and third (>320 °C) peak areas, T_m rise from 271 °C to 293 °C and 378 °C to 391 °C, when POSS content increased from 0% to 13.4%, as seen from **P1** to **P4** in Fig. 4(B). This indicates clearly that incorporation of POSS is beneficial for improving the thermal stability of the polymer.

In general, when heating or combusting POSS-based nanocomposites, the POSS cage can form the thermally stable ceramic-char surface layer which is able to act as a thermal shield by surface re-irradiation and as a barrier to heat or oxygen transfer from flame to the material [47]. Fig. 5 showed the SEM images of residue of cotton fabrics coated with **P1** (Fig. 5(A)) or **P4** (Fig. 5(B)) after burning in air. The obvious difference between Fig. 5(A) and Fig. 5(B) was observed. The fibers in Fig. 5(A) were slim and flaky, while the fibers in Fig. 5(B) were strong and thick. And furthermore, the carbon char and silica particles were observed on the fiber in Fig. 5(B). It can be explained with the formation of a carbon char in oxidative conditions favoured by POSS presence to produce a POSS/carbon char composite layer protecting the underlying polymer and cotton fabrics from oxygen.

3.3. Surface morphology of the coated fabrics

FE-SEM was used to investigate the morphology of the polymers on cotton fabrics and glass substrates. Ov-POSS particles can be dissolved in THF solution and deposited on a slide glass. Fig. 6(A) shows the FE-SEM images of the Ov-POSS deposited on the slide

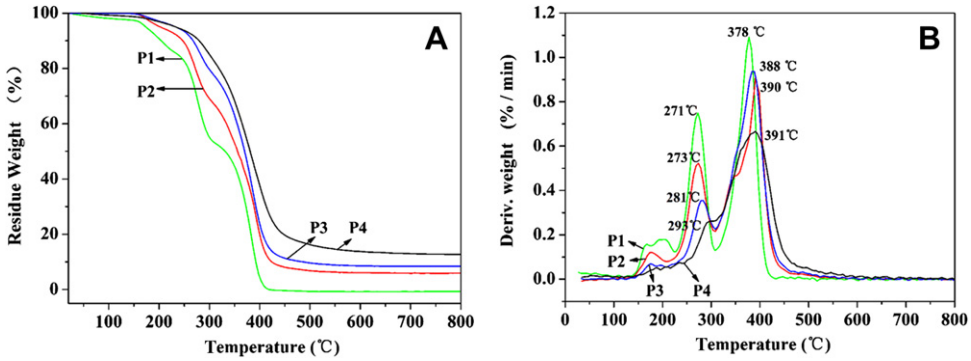

Fig. 4. TG (A) and DTG (B) curves of polymers under nitrogen.

glass which displays that agglomeration size of Ov-POSS is 30–60 nm (seen in the red rectangular) and crystal aggregate size is larger than 1000 nm. The surfaces of fabrics coated with **P1** (Fig. 6 (B)) has no such white nano particles due to the absence of POSS unit in **P1**. In contrast, white particles less than 100 nm are regularly distributed on the surfaces of the cotton fabrics coated with **P2**, **P3** and **P4** (Fig. 6(C)–(E)). Moreover, the quantity of white particles on the surface of cotton fabric treated with **P4** is significantly more than that with **P2** or **P3** due to the highest POSS contents in **P4**.

3.4. Wetting characteristics of the coated fabrics

The hydrophobicities of the coated cotton fabric surfaces were assessed with water contact angle (CA) measurements. In addition, the most important parameter for the movement of water droplets on a surface, the CA hysteresis value was also measured.

Table 2
The effect of POSS content and fluorine content on the wetting behaviors of the coated fabrics.

Polymer coated	POSS ratio (wt%)[a]	Fluorine ratio (wt%)[b]	WCA Hysteresis (°)	Static contact angles (°)		
				Water	Salad oil	Hexadec.[c]
PMMA	0	0	13 ± 3	122 ± 1	84 ± 4	0
P(MMA-POSS)	10.8	0	7 ± 1	142 ± 3	65 ± 2	0
P1	0	43.8	7 ± 1	131 ± 2	125 ± 2	91 ± 1
P2	6.4	42.2	6 ± 1	140 ± 2	127 ± 1	104 ± 3
P3	9.5	38.8	4 ± 1	148 ± 3	138 ± 2	117 ± 2
P4	13.4	25.3	4 ± 2	152 ± 2	144 ± 3	105 ± 2

[a] POSS ratio was obtained from the elemental analyses of Si.
[b] Fluorine ratio was obtained from elemental analyses of F.
[c] Hexadec. is an abbreviation for Hexadecane.

The data summarized in Table 2 show that water CA increases with the increasing of POSS content while water CA hysteresis decreases with it. For liquids with high surface tension, e.g. water, the morphology of hydrophobic solid surface is the decision factor to achieve superhydrophobicity. The water CAs of PMMA (~122°), P(MMA-POSS) (~142°), **P1** (~131°) to **P4** (~152°) in Table 2 show that hydrophobicity of the coated cotton fabrics were improved by the addition of POSS. The surface of the cotton fabrics coated with **P4** exhibits the roughest morphology (seen in Fig. 6(E)) and from which superhydrophobicity achieves, the water CA is higher than 150°, and the CA hysteresis is lower than 5°.

Similarly, the salad oil CAs for samples **P1** to **P4** indicate that the salad oil repellency is also improved by the incorporation of POSS. The salad oil CA increases from ~125° to ~144° when the incorporated POSS content from 0 (**P1**) to 13.4 wt% (**P4**). However, the salad oil CAs for sample PMMA and P(MMA-POSS) (Table 2) show that incorporating POSS in PMMA can't improve the salad oil repellency. This phenomenon could be explained by the well-known Wenzel's Theory [48]. According to the Wenzel's Theory, if the CA of a liquid on a smooth surface is less than 90°, the apparent CA on a rough surface will be smaller, and the higher the roughness, the smaller the apparent CA is; while for a true CA >90°, the CA on a rough surface will be larger, and the higher the roughness, the larger the apparent CA is. The surface of the cotton fabrics coated with PMMA is lipophilic (oil CA <90°), so increasing the surface roughness leads to the higher lipophilicity. The salad oil CA decreases to ~65° when 12.5 wt% POSS incorporated in PMMA. While the surface of the cotton fabrics coated with **P1** is oleophobic (oil CA >90°) due to the fluorine containing segment, increasing roughness of the surface is helpful to improve the oil repellency.

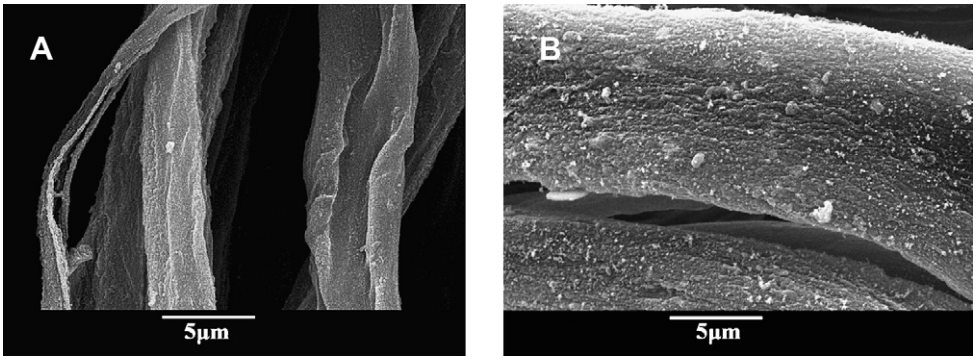

Fig. 5. SEM microphotographs of the coated cotton fabrics after burning in air. (A) cotton fabric coated with **P1**, (B) cotton fabric coated with **P4**.

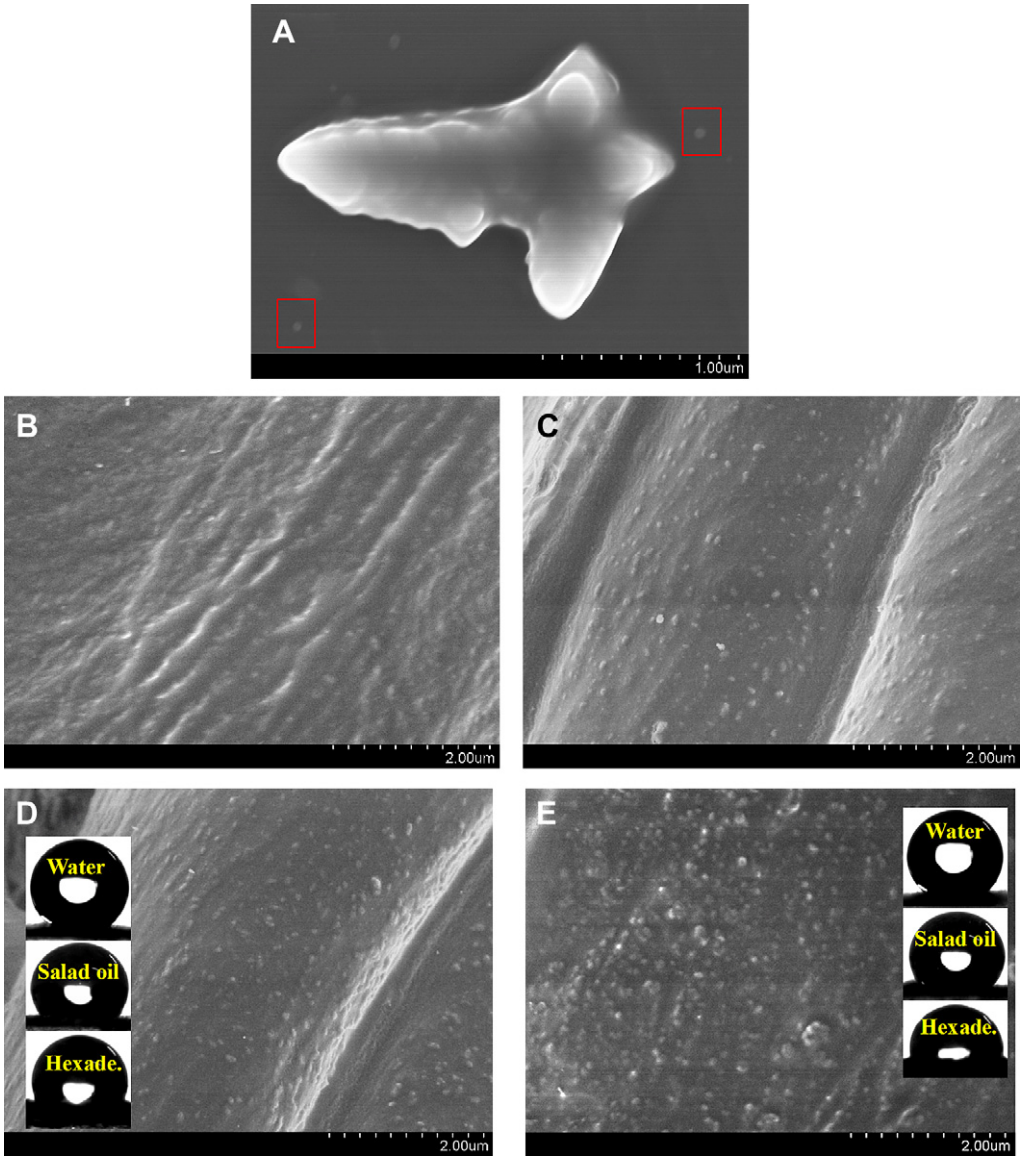

Fig. 6. FE-SEM images of Ov-POSS and coated cotton fabrics surfaces. Insets are photos of liquid droplets on the corresponding samples. (A) Ov-POSS, (B) cotton fabric coated with **P1**, (C) cotton fabric coated with **P2**, (D) cotton fabric coated with **P3**, (E) cotton fabric coated with **P4**.

For the lower surface tension oil, hexadecane (surface tension: 27.4 mN/m, 20 °C), the CAs for samples coated with PMMA and P(MMA-POSS) are only 0° because the polymers are lack of low surface free energy composite. Since the trifluoromethyl group ($-CF_3$) terminated surface has been reported to possess the lowest surface free energy, high oil repellency can be achieved only through a complementary combination of the $-CF_3$ terminal functionality and hierarchical surface roughness [49]. Compared with the hexadecane CA for sample PMMA (0°), the CA for **P1** (~91°) is much higher, which proves that the polymer oil repellency could be achieved by the incorporation of fluorine composite. While meeting the precondition of ensuring enough fluorine, the oleophobicity of the surface could be improved by enhancing the roughness of the surface. So, the hexadecane CAs on the polymers (**P1** to **P3**) treated cotton fabrics increases from ~91° to ~117° with the increase of the POSS content from 0% to 9.5%. But, in the terpolymer, the fluorine content decreases inevitably when POSS content increases. When the fluorine content deceases too much, oleophobicity is poor consequently, so that the hexadecane CA for **P4** coated fabric reduces to ~105°. Based on the influence of the POSS content and fluorine content on the hydrophobicity and oleophobicity of the coated cotton fabrics, it can be concluded that the hydrophobicity and oleophobicity of the hybrid copolymer can be effectively tuned by varying the feed ratio of POSS.

We also measured water CAs of the cotton fabrics coated with the simple physical mixture of P(MMA-$(HFPO)_3$MA) (**P1**) and Ov-POSS (4–15 wt%), and found that the deviation of the CA increased with the increasing of Ov-POSS content. The difference between the minimum and maximum water CAs is more than 30° at 12 wt% and 15 wt% of Ov-POSS content, much higher than that of the cotton fabrics coated with POSS-based terpolymers. Take the sample with 12 wt% POSS as example, the minimum water CA is only ~112°, while the maximum one is ~145°, which are too uneven to obtain the uniform data. Fig. 7 shows the morphology of **P1**/Ov-POSS mixture with different POSS content. The different extent of phase separation was observed in each sample. It's interesting to note that butterfly-like POSS aggregate structure appeared with 15 wt% POSS

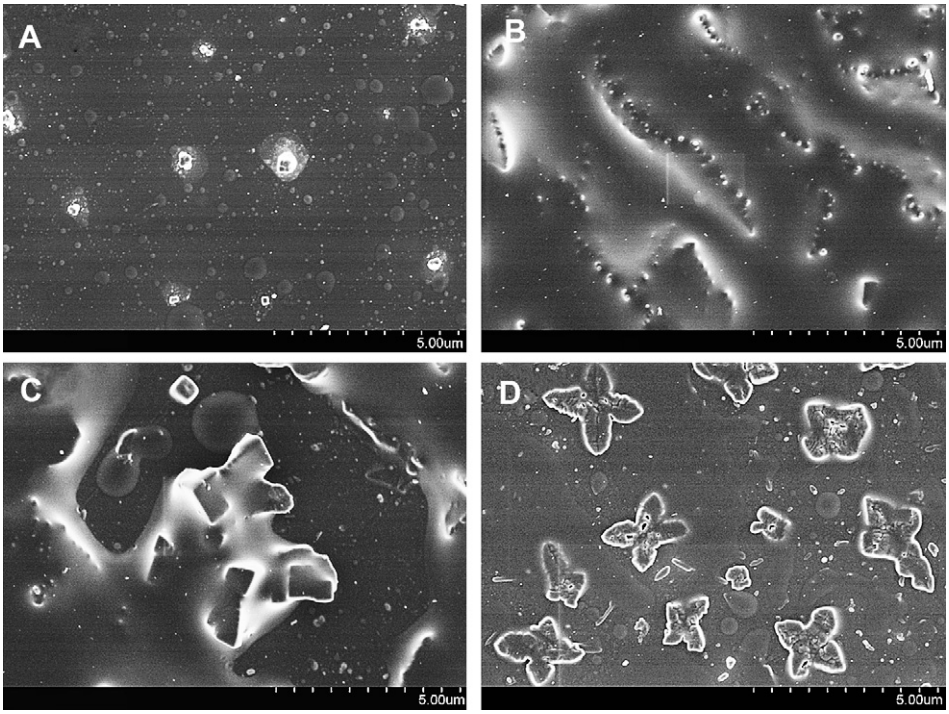

Fig. 7. FE-SEM images of **P1**/Ov-POSS mixtures with different POSS weight content on glass substrates. (A): 4%; (B): 8%; (C): 12%; (D): 15%.

in the mixture, seen in Fig. 7(D). The poor miscibility of POSS and P(MMA-(HFPO)$_3$MA) resulted in uneven distribution of both surface energy and morphology, which is the main reason for the uneven hydrophobicity of the mixture coated cotton fabrics surfaces. In view of the hydrophobicity distribution, the terpolymer far outweighs the physical mixture.

3.5. Surface chemical composition of the *P3* coated fabric

The surface chemical composition of it was analyzed by XPS analysis. As shown in Fig. 8(A), Si 2s, Si 2p, C 1s, O 1s, F 1s and F 2s peaks were detected at around 150, 100, 285, 535, 690 and 30 eV, respectively. The high-resolution XPS spectrum of carbon 1s was shown in Fig. 8(B) which was fitted with seven subpeaks having equal width corresponding to $-CF_3$ at 293.6 eV, $-CF_2$ at 291.8 eV, $-CF$ at 290.7 eV, $-C{=}O$ at 288.4 eV, $C-O$ at 286.1 eV, $C-C$ at 284.8 eV and $C-Si$ at 284.1 eV [43,50]. The XPS quantification in atomic concentration has been carried out taking into account the individual peak areas and the corresponding atomic sensitivity factors (ASF). The relative atomic concentration of *i* element (C_i) can be calculated using the equation:

$$C_i = \frac{I_i/ASF_i}{\sum_j I_j/ASF_j} \quad (1)$$

The ASF values provided here for Si 2p, C 1s, O 1s, and F 1s are 0.29, 0.25, 0.66 and 1.00, respectively. The calculated atom concentrations of F and C in the outermost surface coated with **P3** are 46.5% and 39.1%, respectively. The atomic ratio of F/C is 1.19 significantly higher than the corresponding bulk atomic ratio (F/C, 0.59) of **P3**, indicating a strong surface enrichment of fluorinated segment. The atomic ratio of F/C for **P1** and **P4** coated cotton fabric are also obtained by XPS measurement, which is 1.23 and 1.06, respectively. Among all polymer-coated cotton fabrics, **P3** coated cotton fabric shows high oil repellency. The atomic ratio of F/C for **P3** is close to that of **P1** and higher than that of **P4**, which means the enrichment fluorine segment on the rougher surface plays key role in achieving high oleophobicity.

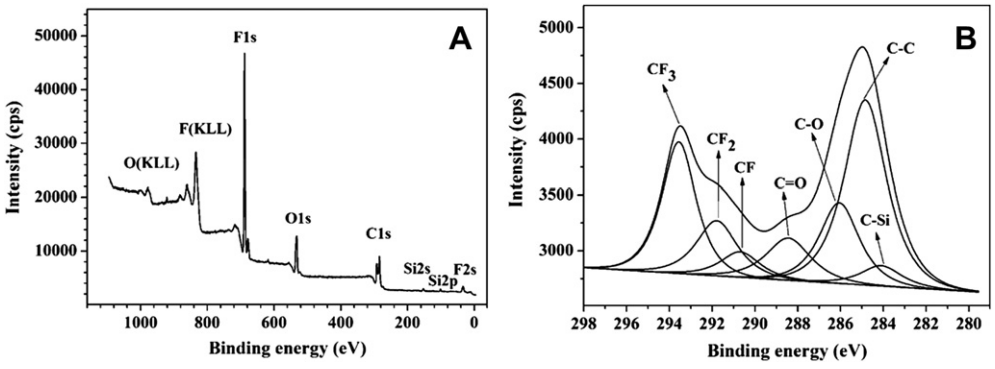

Fig. 8. XPS spectra of the cotton fabrics surface coated with **P3**. (A) Wide-scan survey spectrum for all elements, (B) High-resolution spectrum for C1s signals.

4. Conclusions

A new class of water and oil repellent terpolymers containing POSS and fluoropolyether segments were prepared and characterized successfully. With the increasing of the POSS content in our research range, better thermal stability and hydrophobicity of the terpolymer were obtained. The hydrophobicity and oleophobicity of the terpolymer could be adjusted by controlling the feed ratio of Ov-POSS. The cotton fabrics coated with the terpolymers could achieve superhydrophobicity and high oleophobicity. Moreover, the POSS segment in the terpolymer mitigated the burning of the coated cotton fabrics in air to some extent by formation the protective char layer. Finally, the terpolymer is potential to be endowed other functional groups from the unreacted vinyl groups in the POSS segments, and thus to be developed for various potential applications.

Acknowledgements

We are grateful to the Program for Changjiang Scholars and Innovative Research Team in University (No. IRT0526) and Shanghai Municipal Scientific Committee (09PJ1400800) for the financial support.

References

[1] Zhang L, Zhou Z, Cheng B, DeSimone JM, Samulski ET. Langmuir 2006;22:8576–80.
[2] Zhang X, Shi F, Niu J, Jiang Y, Wang Z. J Mater Chem 2008;18:621–33.
[3] Okano T, Kikuchi A, Sakurai Y, Takei Y, Ogata N. J Control Release 1995;36:125–33.
[4] Johansson A, Calleja M, Dimaki MI, Rasmussen P, Boggild P, Boisen A. Sensor Lett 2004;2:117–20.
[5] Wu X, Zheng L, Wu D. Langmuir 2005;21:2665–7.
[6] Ming W, Wu D, van Benthem R, de With G. Nano Lett 2005;5:2298–301.
[7] Choi S-J, Suh KY, Lee HH. Nanotechnology 2008;19:275305–10.
[8] Liu H, Feng L, Zhai J, Jiang L, Zhu DB. Langmuir 2004;20:5659–61.
[9] Zhai L, Cebeci FC, Cohen RE, Rubner MF. Nano Lett 2004;4:1349–53.
[10] Tuteja A, Choi W, Ma ML, Mabry JM, Mazzella SA, Rutledge GC, et al. Science 2007;318:1618–22.
[11] Salima Saïdi, Frédéric Guittard, Claude Guimon, Géribaldi S. J Appl Polym Sci 2006;99:821–7.
[12] Martinelli E, Glisenti A, Gallot B, Galli G. Macromol Chem Physic 2009;210:1746–53.
[13] Ghosh N, Bajoria A, Vaidya AA. ACS Appl Mater Interfaces 2009;1:2636–44.
[14] Trombetta T, Iengo P, Turri S. J Appl Polym Sci 2005;98:1364–72.
[15] Coulson SR, Woodward IS, Badyal JPS, Brewer SA, Willis C. Chem Mater 2000;12:2031–8.
[16] Chen W, Fadeev AY, Hsieh MC, Oner D, Youngblood J, McCarthy TJ. Langmuir 1999;15:3395–9.
[17] Kim TI, Tahk D, Lee HH. Langmuir 2009;25:6576–9.
[18] Lee YJ, Kuo SW, Huang CF, Chang FC. Polymer 2006;47:4378–86.
[19] Kannan AG, Choudhury NR, Dutta N. ACS Appl Mater Interfaces 2009;1:336–47.
[20] Huang KW, Tsai LW, Kuo SW. Polymer 2009;50:4876–87.
[21]. Ni Y, Zheng SX. Macromol Chem Phys 2005;206:2075–83.
[22] Raftopoulos KN, Pandis C, Apekis L, Pissis P, Janowski B, Pielichowski K, et al. Polymer 2010;51:709–18.
[23] Huang CF, Kuo SW, Lin FJ, Huang WJ, Wang CF, Chen WY, et al. Macromolecules 2006;39:300–8.
[24] Yang BH, Xu HY, Li C, Guang SY. Chin Chem Lett 2007;18:960–2.
[25] Li HY, Yu DS, Zhang JY. Polymer 2005;46:5317–23.
[26] Zhang H, Shin Y, Yoon K, Lee D. Eur Polym J 2009;45:40–6.
[27] Randriamahefa S, Lorthioir C, Guégan P, Penelle J. Polymer 2009;50:3887–94.
[28] Chen JH, Yao BX, Su WB, Yang YB. Polymer 2007;48:1756–69.
[29] Bian Y, Mijovic J. Polymer 2009;50:1541–7.
[30] Paul R, Karabiyik U, Swift MC, Hottle JR, Esker AR. Langmuir 2008;24:4676–84.
[31] Misra R, Alidedeoglu AH, Jarrett WL, Morgan SE. Polymer 2009;50:2906–18.
[32] Bharadwaj RK, Berry RJ, Farmer BL. Polymer 2000;41:7209–21.
[33] Iacono ST, Budy SM, Mabry JM, Smith DW. Macromolecules 2007;40:9517–22.
[34] Xu JW, Li X, Cho CM, Toh CL, Shen L, Mya KY, et al. J Mater Chem 2009;19:4740–5.
[35] Zeng K, Wang L, Zheng SX, Qian XF. Polymer 2009;50:685–95.
[36] Ellis DA, Mabury SA, Martin JW, Muir DCG. Nature 2001;412:321–4.
[37] Keil DE, Mehlmann T, Butterworth L, Peden-Adams MM. Toxicol Sci 2008;103:77–85.
[38] Malinverno G, Colombo I, Visca M. Regul Toxicol Pharmacol 2005;41:228–39.
[39] Krupers M, Slangen PJ, Moller M. Macromolecules 1998;31:2552–8.
[40] Puukilainen E, Koponen HK, Xiao Z, Suvanto S, Pakkanen TA. Colloids Surf A 2006;287:175–81.
[41] Yarbrough JC, Rolland JP, DeSimone JM, Callow ME, Finlay JA, Callow JA. Macromolecules 2006;39:2521–8.
[42] Fabbri P, Messori M, Montecchi M, Pilati F, Taurino R, Tonelli C, et al. J Appl Polym Sci 2006;102:1483–8.
[43] Vaidya A, Chaudhury MK. J Colloid Interface Sci 2002;249:235–45.
[44] Paleta O, Paleek J, Michálek J. J Fluorine Chem 2002;114:51–3.
[45] Xu HY, Yang BH, Wang JF, Guang SY, Li C. J Polym Sci Part A Polym Chem 2007;45:5308–17.
[46] Hussain H, Mya KY, Xiao Y, He CB. J Polym Sci Part A Polym Chem 2008;46:766–76.
[47] Bourbigot S, Duquesne S, Jama C. Macromol Symp 2006;233:180–90.
[48] Feng X, Jiang L. Adv Mater 2006;18:3063–78.
[49] Aulin C, Yun SH, Wågberg L, Lindström T. ACS Appl Mater Interfaces 2009;1:2443–52.
[50] Fabbri P, Messori M, Montecchi M, Nannarone S, Pasquali L, Pilati F, et al. Polymer 2006;47:1055–62.